Journal of Engineering and Computer Sciences
Qassim University, Vol. 5, No. 1, pp. 77-92 (January 2012/Safar 1433H)

Numerical Simulation of Mixed Convection from Longitudinal Fins in a Horizontal Rectangular Channel

A. S. Alosaimy
Mechanical Engineering Department, Faculty of Engineering,
Taif University, Taif 21974, Saudi Arabia
alosaimy@yahoo.com

(Received 18/4/2011; accepted for publication 4/11/2011)

ABSTRACT. A numerical investigation was undertaken to investigate heat transfer in three-dimensional laminar mixed convection heat transfer from longitudinal fins in a horizontal rectangular channel. Numerical simulations were conducted at different fin spacing, Reynolds number of 1500 and modified Rayleigh number of 4 x 10^7 and 2x 10^8 for fin to channel height ratios of 0.5 and 0.25. Validity of the modelling technique is verified by comparing computational results with corresponding experimental data from literatures. The numerical model is able to simulate the mixed convective flow through a rectangular channel subjected to constant heat flux heating boundary conditions. The predicted heat transfer coefficient and local Nusselt number distribution shows a good agreement with the experimental results and its improvement with higher channel height ratio at the expense of increased pressure drop across the longitudinal fins.

Keywords: longitudinal fins, mixed convection, Numerical simulation.

NOMENCLATURE

A	channel cross sectional area, m^2
C_p	Specific heat, kJ/ kg
f	friction factor
D_h	channel hydraulic diameter, 4A/P, m
G	gravitational acceleration, m/s^2
h_{av}	average convective heat transfer coefficient, W/m^2K
H	channel height, m
H_f	fin height, m
k	air thermal conductivity, W/m K
L	channel heated length, m
L_m	length of te model, m
Nu_{av}	average Nusselt number, $Nu_{av}=h_{av}D_h/k$
Nu_{wx}	local Nusselt number, $Nu_{wz}= q_{con} D_h/ ((T_{wx}-T_{in}) k)$
p	pressure, Pa and perimeter, m
q_{con}	Convection heat flux, W/m^2
Ra^*	modified Rayleigh number, $Ra^*=(g\beta q_{con}D_h^4)/(k\,\alpha\upsilon)$
Re	Reynolds number, $Re= u_{in} D_h/\upsilon$
S	fin spacing, m

T	temperature, K
T_{wx}	local wall temperature, K.
u	u-velocity componente, m/s
U	streamwise bulk velocity, m/s
v	v-velocity component, m/s
W	half channel width, m
x_w	axial distance along heated wall,m
x	x-coordinate direction
y	y-coordinate direction
z	z-coordinate direction

Greek letters

α	thermal diffusivity, m^2/s
β	thermal expansion coefficient, 1/K
υ	kinematic viscosity, m^2/s
ρ	density, kg/m^3
τ	shear stress, N/m^2

Subscripts

av	average
f	fin
in	inlet
w	wall
x	x-direction

1. INTRODUCTION

Fins are widely used to enhance convective heat transfer in engineering applications such as solar collectors, heat exchangers, HVAC industries and substation transformers. Many types of flat fins have been presented by Shah and Sekulic' [1]. The most common were the plain, wavy and interrupted and the first types of fins were used in those applications in which the pressure drop is quite low.

Krikkis and Razelos [2] presented correlations for optimum dimensions of longitudinal rectangular and triangular radiating fins with mutual irradiation. Kasbioui *et al.* [3] studied the heat transfer and fluid flow by mixed convection in a vertical rectangular cavity containing adiabatic partitions attached to the heated wall. The parameters of Rayleigh number, Reynolds number, aspect ratio of the cavity and the aspect ratio of the micro cavities were considered. The results indicated that the heat exchange between the system and the external medium, through the cold wall and the upper vent, were considerably affected by the presence of the partitions. Experiments were performed by Maughan [4] to determine secondary flow development and Nusselt number distributions for laminar mixed convection in the thermal entry region of a parallel plate channel heated uniformly from below. Longitudinal distributions of the local Nusselt number initially followed forced convection. Subsequent mixing associated with the development of secondary flow caused Nusselt numbers to rise to an initial maximum before decreasing slightly and assuming a fully developed value. Tiwade and Pathare [5] investigated experimentally the performance of continuous longitudinal fins solar air heater. They demonstrated that the addition of continuous longitudinal fins to the upper or bottom side of the absorber plate improves the heat transfer rate. Also, it is found that effective heat transfer coefficient is maximum for the smallest pitch of the longitudinal fins, in addition the friction factor and pressure drops are found lowest with largest Reynolds number.

Mixed convection heat transfer from longitudinal fins inside a horizontal channel has been investigated by Dogan and Sivrioglu [6] in the natural convection dominated region for a wide range of Rayleigh numbers and different fin heights and spacing. An experimental parametric study was made to investigate effects of fin spacing, fin height and magnitude of heat flux on mixed convection heat transfer from rectangular fin arrays heated from below in a horizontal channel. The optimum fin spacing to obtain maximum heat transfer has also been investigated. Experiments were conducted for Reynolds number of 250 and modified Rayleigh numbers ranging between 3×10^7 and 6×10^8. The results showed that the dimensionless optimum fin spacing to channel height (S/H) which yields the maximum heat transfer is between $S/H = 0.08$ and $S/H = 0.12$. Results also show that optimum fin spacing depends on modified Rayleigh number and fin height. They conducted the same experiments with different inlet conditions [7]. Experiments were conducted for Reynolds number of 1500 and modified Rayleigh numbers ranging between 3×10^7 and 8×10^8. The results showed that the dimensionless optimum fin spacing

to channel height (S/H) which yields the maximum heat transfer is between S/H = 0.08 and S/H = 0.09.

Numerical investigation of shrouded fin array under combined free and forced convection was studied by Al-Sarkhi *et al.* [8]. It is concluded that Nusselt number is significantly enhanced by the effects of buoyancy in the mixed convection regime.

Biswas et al [9] carried out numerical computation of laminar mixed convection flows and heat transfer in a rectangular channel with geometrical fin configuration to represent a part of gas-liquid, fin-pipe cross flow heat exchanger (gas side). The mixed convection condition was characterized by buoyancy induced secondary flows leading to increase the vortex strength and improve the heat transfer. Wu and Perng [10] studied the simulation of laminar mixed convection in a horizontal channel containing heated blocks. The effect of an oblique plate on the heat transfer improvement was obtained. These results show that the installation of the plate can improve the heat transfer and flow field instability.

Yalcin et al [11] investigated the effects of clearance parameters on the steady-state heat transfer. A finite volume based CFD code was used in order to solve the three-dimensional elliptic governing equations. The numerical results have been compared to existing experimental values from the literature and the comparison showed a good agreement. It was found that the heat transfer coefficient increases with the increase in the clearance parameter and it approaches to the value of heat transfer coefficient obtained for un-shrouded fin arrays. Four basic fins of the plate-fin heat exchangers have been modelled and simulated by Zho and Lee [12]. Three-dimensional numerical simulations on the flow and heat transfer in the four fins were investigated and carried out at laminar flow regime. Validity of the modelling technique was verified by comparing computational results with both corresponding experimental data and three empirical correlations from literatures.

The objective of the present study is to perform numerical three-dimensional simulation of mixed convection heat transfer from longitudinal fin arrays in a horizontal channel. The validity of the calculations was verified by comparing the computational results with corresponding experimental data of Dogan and Sivrioglu [7]. All computations were performed using ANSYS FLUENT 12- CFD code.

2. MODEL DESCRIPTION AND SIMULATION

The problem analyzed in this study involved convective heat transfer in a rectangular duct with longitudinal fins of 1 mm thickness each attached to the bottom wall. The computational domain of the physical problem is shown in Figure 1. The problem is modeled using one face as symmetric plane along the flow. By exploiting the symmetry of the flow field in the spanwise direction, and the width of the computational domain is reduced to half of the actual width of the duct (W = 0.15 m) with channel height H of 0.10 m. The length of the model L_m is equal to 1.0 m and consists of unheated entrance region L_{in} of 0.20 m, heated wall involving longitudinal fins L of 0.60 m and finally the unheated exit region L_{ex} of 0.20 m. Two fin heights H_f are considered in this investigation to satisfy fin height ratios H_f/H of

0.25 and 0.50. Thin aluminum fins of 1mm thick are considered with different spacing S.

Calculations were carried out using inlet Reynolds number of 1500 and modified Rayleigh number Ra* of 4 x 10^7 and 2x 10^8 for fin to channel height ratios H_f/H of 0.5 and 0.25 respectively. In the experimental results of Dogan, M., Sivrioglu. [7], it has been shown that values of Richardson number for fin heights H_f/H= 0.25 and 0.50 at different fin spacing ratios indicates the dominant effect of mixed convective heat transfer for these conditions experimental.

The steady laminar three-dimensional momentum and energy equations are solved numerically (using finite volume scheme) together with the mass conservation equation to simulate the thermal and the flow fields. The equations are expressed in the Cartesian tensor notation and given by:

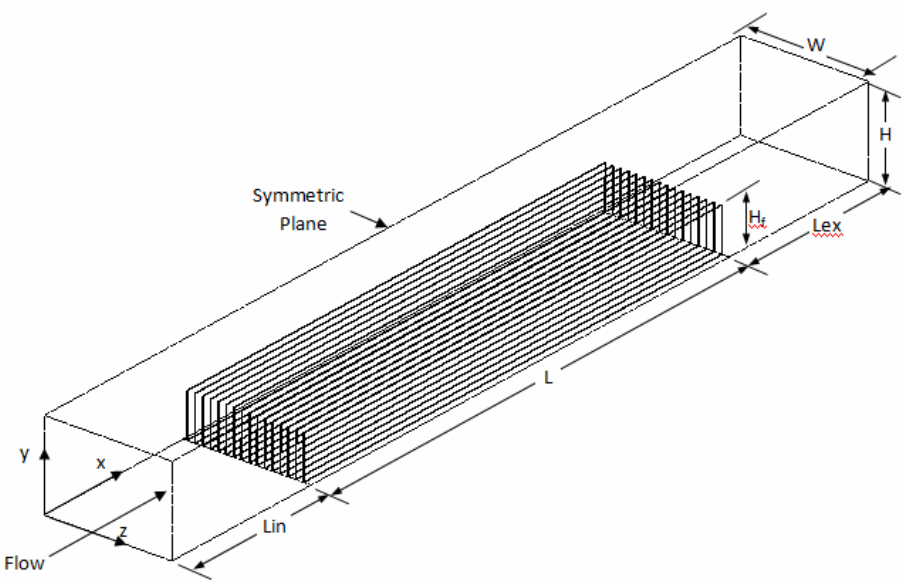

Fig.(1). Three-dimensional computational model.

Mass conservation equation:

$$\frac{\partial}{\partial x_i}(\rho u_i) = 0 \tag{1}$$

Momentum equation

$$\frac{\partial}{\partial x_j}(u_i u_j) = -\frac{\partial p}{\partial x_i} + \frac{\partial}{\partial x_j}\tau_{ij} + \rho_{in} g_i \beta (T - T_{in}) \tag{2}$$

where

$$\tau_{ij} = \mu\left(\frac{\partial u_i}{\partial x_j} + \frac{\partial u_j}{\partial x_i} - \frac{2}{3}\delta_{ij}\frac{\partial u_l}{\partial x_l}\right) \quad (3)$$

Energy Equation:

$$\frac{\partial}{\partial x_j}\left(\rho C_p u_j T\right) = \frac{\partial}{\partial x_j}\left(k\frac{\partial T}{\partial x_j}\right) \quad (4)$$

Here the coordinate direction is referred as x_i $(x_i = x, y, z)$, and the velocity component in such direction is represented by u_i $(u_i = u, v, w)$.

In the present study all computations were performed using ANSYS FLUENT 12- CFD code. The simulation of three-dimensional flow was adopted with assumption of steady laminar flow conditions. The momentum and energy equations governing the fluid motion and the energy transport for incompressible flow were solved through the Finite Volume Method, using a three-dimensional formulation with the SIMPLEC-algorithm for pressure velocity coupling.

The mesh consisted of 247197 binary nodes and 65216 quadrilateral wall faces at heated rib-channel interface. The interior faces were counted as 59792 quadrilateral in the ribs and 2596146 (triangular) in the channel area. In total 1310871 mixed cells were generated for the entire model. The exterior walls of the channel were set as isothermal and the bottom wall was subjected to a constant heat flux. Average values of heat transfer coefficient are evaluated from the following expression:

$$h_{av} = \frac{1}{A}\int h dA \quad (5)$$

3. RESULTS AND DISCUSSION

3.1 Heat transfer coefficient, local temperature and Nusselt number

The comparison between the predicted values and the experimental results published by Dogan, M., Sivrioglu [7] are presented in Figures 2-4. The Effect of fin spacing on the variation of average convection heat transfer coefficient h_{av} is presented in Figure2. It is shown that the predictions are able to catch the optimum of the h_{av} at fin spacing S= 8 mm as well as the experimental results. However, discrepancies between the present numerical predictions and the published results are evident in both cases of modified Rayleigh number. The average heat transfer is overestimated except for fin spacing greater than 12 mm at Ra* of 4 x 10^7. The maximum deviation between the numerical and the experimental results is 7.6% compared with an uncertainty of around ±6% for the experimental results.

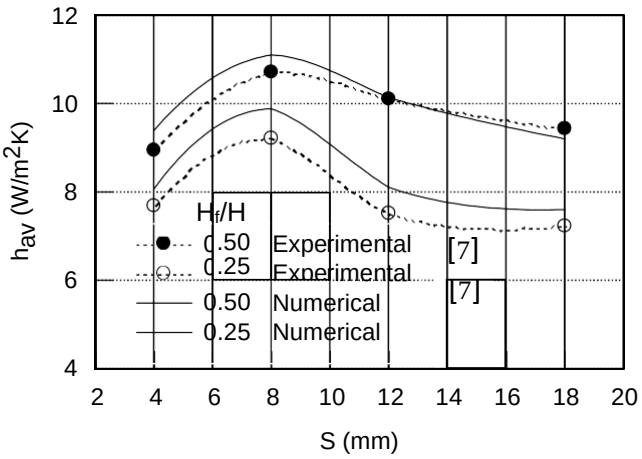

Fig.(2). Variation of average convection heat transfer coefficient with fin Spacing.

The variation of dimensionless temperature and local Nusselt number distributions with the main flow direction are shown in Figures 3 and 4 for different modified Rayleigh number , fin heights H_f/H= 0.25 and 0.50 for the same fin spacing ratio S/H=0.08. It is seen that the numerical and the experimental results have the same trend and the dimensionless temperature is underestimated up to 80% of the heated wall length. This results are associated with higher predicted local Nusselt number, and the predicted maximum dimensionless temperature is close to the experimental value for fin height H_f/H= 0.50 at modified Rayleigh number Ra* of 4×10^7.

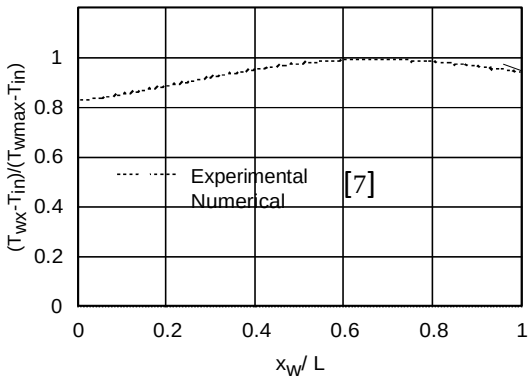

(a)

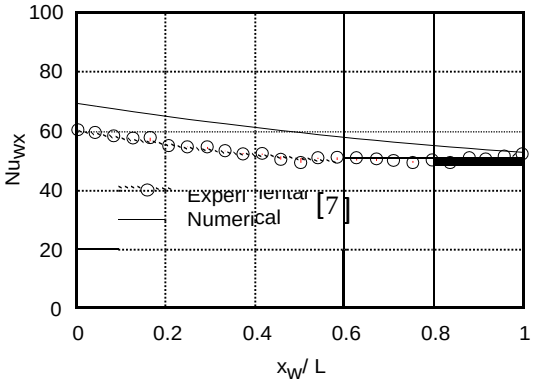

(b)

Fig.(3). (a) Variation of the temperature distribution and (b) variation of local Nusselt number with the main flow direction (S/H=0.08 and Hf /H=0.25).

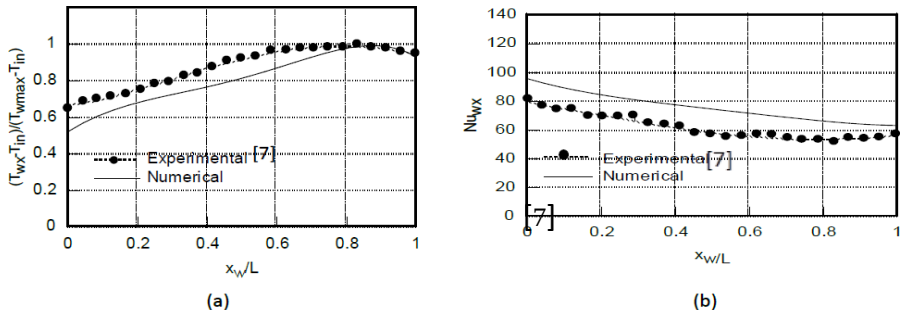

Fig. (4). (a) Variation of the temperature distribution and (b) variation of local Nusselt number with the main flow direction (S/H=0.08 and Hf /H=0.50)

3.2 Temperature profiles

The temperature profiles on the heated bottom wall with 16 Longitudinal fins is shown in Figure (5). It is clear that the temperature increases in the streamwise flow direction. The temperature at the side wall of the channel increases near the exit section. This may be attributed to the very low velocities at the corner of the channel located between the bottom and the side wall. [7]

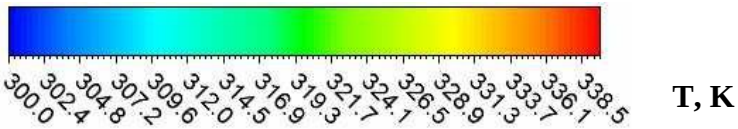

Side wall

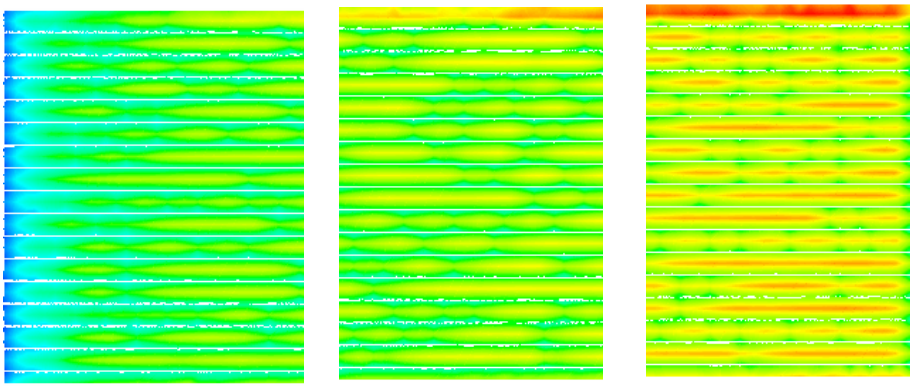

Symmetric plane

Near Inlet Middle Section Near Exit

Fig. (5). Temperature profiles on the heated wall (S/H=0.08 and H_f/H=0.50).

The temperature profiles across and along flow symmetric plane are shown in Figures (6 and 7) for the case of S/H=0.08 and H_f/H=0.50. It is clear that temperature gradients are evident due to heat transfer from bottom wall and the walls of fins. Higher temperatures are shown between ribs and in particular at the proximity of the bottom wall. A large region of the duct outside the fin grooves is occupied with air having the same temperature of inlet condition. This region is extended along the flow up to the middle section of the duct.

3.3 Velocity profiles

The velocity vectors plots along the flow and velocity component v at symmetric plane are shown in Figures(8 and 9). The flow velocities at the upper region, which is not occupied by fins, shows a lower values compared with the velocities at the region between fins. In addition, such region reaches the fully developed profile of streamwise velocities as shown in Figure (10). The peak streamwise velocity tends to have a maximum value at the central section of the duct. The magnitudes of the v velocity components near the inlet section of the duct exhibits negative values to indicated a downward flow at this region. This is attributed to the weak effect of heat transfer at the inlet section of the duct to force the air upward due to low temperature as presented in Figure (8). However, due to the higher temperature near the exit of the duct, the cross flow velocity shows higher positive values between the fins except a small region close to the sidewall of the duct.

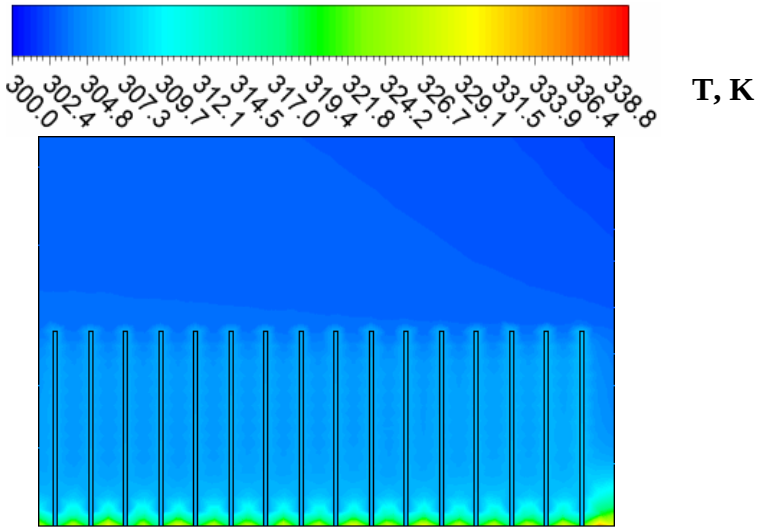

Fig. (6). Temperature profiles across the flow at xw/L =0.5 (S/H=0.08 and Hf/H=0.50).

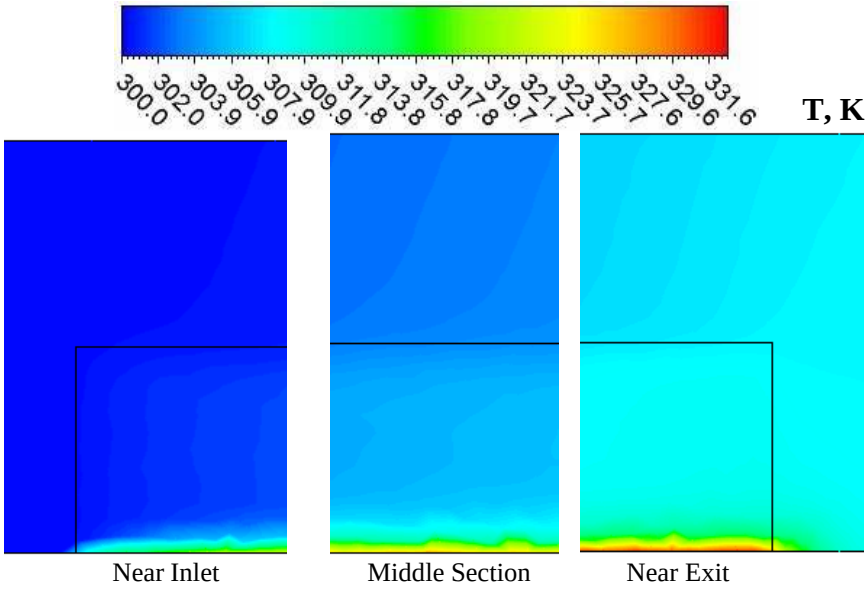

Fig. (7). Temperature profiles at symmetric plane (S/H=0.08 and Hf/H=0.50).

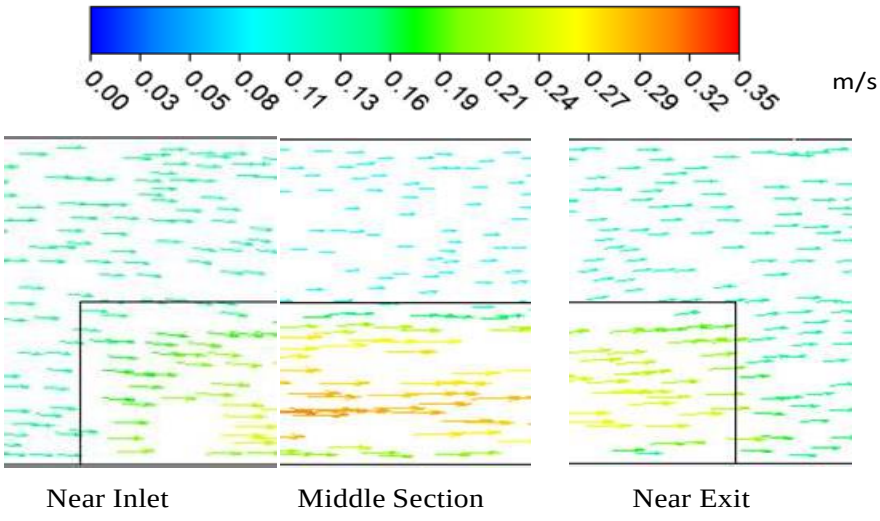

Fig.(8). Velocity vectors plots along the flow at Symmetric plane (S/H=0.08 and Hf/H=0.50).

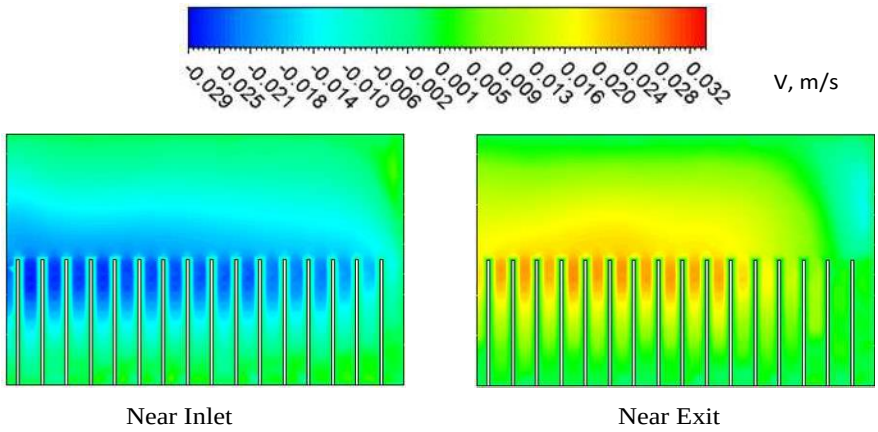

Fig.(9). Velocity profiles across the flow in y-direction (S/H=0.08 and Hf/H=0.50).

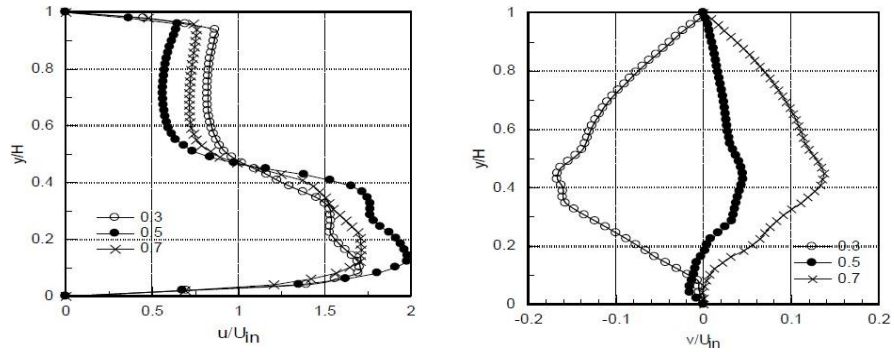

Fig.(10). Velocity distributions at symmetric plane (S/H=0.08 and Hf/H=0.50).

3.4 Friction factor

The pressure drop Δp is defined as the calculated difference between the channel inlet and the channel exit of the model, and the friction factor f, which measures the dimensionless pressure drop, is given by:

$$f = \frac{\Delta p}{\frac{1}{2}\rho U^2}\left(\frac{D_z}{4L_{cs}}\right) \quad (6)$$

The effect of fin spacing (S/H) on the friction factor for fin to channel height ratios (H_f/H) of 0.25 and 0.5 are shown in Figure 11. It is noticed that, the friction factor increases significantly with decreasing spacing ratio and increasing the channel height ratios. This is attributed to the flow resistance generated by the presence of longitudinal fins. The number of fins for (S/H) =0.04, 0.08 and 0.12 are

59, 32 and 12 respectively and more flow resistance and hence pressure drop are expected for higher number of fins or lower values of channel spacing to height ratio.

By investigating Figures (2 and 11), it is seen that the average convection heat transfer coefficient can be improved with higher channel height ratio at the expense of increased pressure drop across the longitudinal fins. The results of calculations showed that, at fin spacing (S/H)=0.08, the average heat transfer coefficient is increase by 12.3% with increasing fin heights (Hf/H) from 0.25 to 0.5. This improvement is associated with an increase in pressure drop by 23.1%.

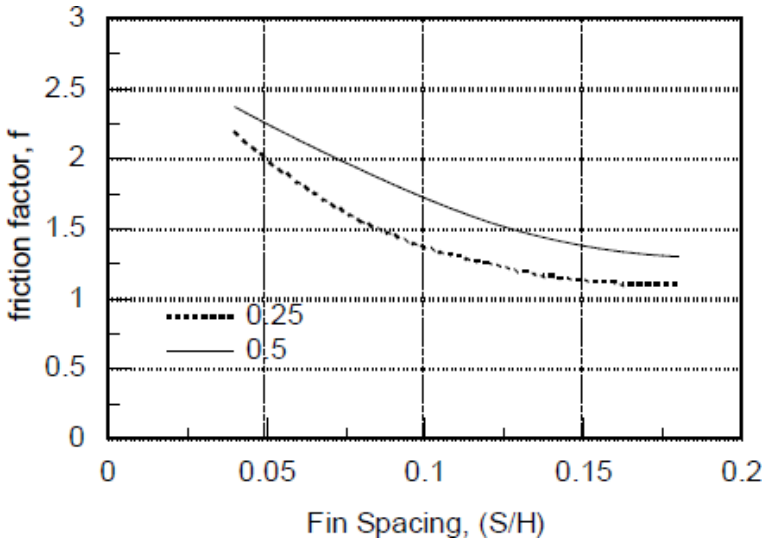

Fig. (11). Effect of fin spacing on the friction factor.

4. CONCLUSIONS

Results from numerical simulations of three-dimensional laminar mixed convection heat transfer from longitudinal fins in a horizontal rectangular channel are validated by experimental work given in literature. Numerical simulations are conducted at Reynolds number of 1500 and modified Rayleigh number of 4×10^7 and 2×10^8 for fin to channel height ratios of 0.5 and 0.25 respectively. The following conclusions may be drawn:

1- The predicted average convection heat transfer coefficient at various configurations of fin spacing and height ratios shows a good agreement with the experimental results.

2- The streamwise velocities between fins reached the fully developed profile and the heating of bottom wall affected the direction of cross flow velocity component downstream of channel inlet section.

3- The friction factor of three-dimensional laminar mixed convection heat transfer from longitudinal fins is significantly increased with decreasing spacing ratio and increasing the channel height ratios.
4- The average convection heat transfer coefficient can be improved with higher channel height ratio at the expense of increased pressure drop across the longitudinal fins.

5. REFERENCES

[1] Shah, D. and Sekulic', D. P., *Fundamentals of heat exchanger design*, Page 699, John Wiley & Sons, Inc., 2003.

[2] Krikkis R.N.و and Panagiotis R., "Optimum Design of Space craft Radiators with Longitudinal Rectangular and Triangular Fins", *J. Heat Transfer*, Vol.124, (2002), pp. 805-811.

[3] Kasbioui, E.K., and Lakhal, M. H., "Mixed convection in rectangular enclosures with adiabatic fins attached on the heated wall", *Engineering Computations*, Vol. 20 No. 2, (2003), pp.152 – 177.

[4] Maughan, J. R. "An experimental and numerical investigation of mixed convection in channels and the application of extended surfaces for heat transfer enhancement", *Journal of Engineering Physics and Thermophysics*, Vol. 19, No. 2, pp. 1011-1015.

[5] Tiwade, P. C., and Pathare, N.R., "Experimentation and performance analysis on continuous longitudinal fins solar air heater", *2nd International Conference on Engineering and Technology (ICETET)*, (2009), pp. 1047-1051.

[6] Dogan, M., and Sivrioglu, M., "Experimental investigation of mixed convection heat transfer from longitudinal fins in a horizontal rectangular channel: In natural convection dominated flow regimes", *Energy Conversion and Management*, Vol. 50, No. 10, (2009), pp. 2513- 2521.

[7] Dogan, M., and Sivrioglu, M., "Experimental investigation of mixed convection heat transfer from longitudinal fins in a horizontal rectangular channel", *International Journal of Heat and Mass Transfer* Vol. 53, (2010), pp. 2149-2158.

[8] Al-Sarkhi, A. Abu-Nada, E., Akash, B. A. and Jaber, J. O., "Numerical investigation of shrouded fin array under combined free and forced convection", *Int. Commun. Heat Mass Transfer*, Vol. 30, (2003), pp. 435–444.

[9] Biswas, G., Mitra, N. K., and Fiebig, M., "Computation of laminar mixed convection flow in a rectangular duct with wing-type built-in obstacles", AIAA, *Thermophysics, Plasmadynamics and Lasers Conference*, San Antonio, TX, (1988), pp. 27-29.

[10] Wu, H. W., and Perng, S. W., "Effect of an Oblique Plate on the heat transfer enhancement of mixed convection over heated blocks in horizontal channel", *International Journal of Heat Transfer*, Vol. 42, (1999), pp. 1217-123.

[11] Yalcin, H. G., Baskaya, S., and Sivrioglu, M., "Numerical analysis of natural convection heat transfer from rectangular shrouded fin arrays on a horizontal surface", *Int. Commun. Heat Mass Transfer* Vol. 35, (2008), pp. 299–311.

[12] Zho, Y., and Lee, Y., "Three-dimensional numerical simulation on the laminar flow and heat transfer in four basic fins of plate-fin heat exchangers", *J. Heat Transfer*, Vol. 130, No. 11, (2008), pp. 111-122.

المحاكاة العددية لانتقال الحرارة بالحمل المختلط من زعانف طولية في قناة أفقية مستطيلة

علي العصيمى

Jáç-9zmn á=ç.zn áZrgJn – α;,an ázA,ç – á¥ınµn á=rs á=Z-ş,Z=Jn á¥ınµn pme

alosaimy@yahoo.com

Eم١١٠٢L١١L٤ ¾,÷z١› 5se ؛ م١١٠٢L٤L٨١ ¾,÷z١› م2eF

ملخص البحث ك õ,se ¾ ã=›9b ¤í,>¿› £1=zSk 5Q£,i õ,k.£k ل,¤=ík ÷zş› ãi-2> ãwk,د ¥k.ci y 2¤›
½i «,é,mSk ¿a ã¤1=s Q=e 2s> ai-22»k õ,s,Zk 5Q> y 2eو ك¸ ¤¦,e, @é2=› د,2iek ã=i5i ã=¤éí ã1=ð=ma
ãşms›و ن9=1a ٠٠٢و ,í9=1a ٠٤ ,œ,2e ل22Sk a=1i, Qe, Q=e 2s>و ٠٠٥١ ز2›9si, Qe, 2s>و ¤í,>¿»k
ل5s ¿a o,s,Zk c91wk ã=ek2Qa ¿a @¤z=»k y 2eو ك٠{٥٢ 9i ٠{٥ ¿a õ,s¤»k ع,¤;,k 9i ¤í,>¿»k ع,¤;,k
¿a,íz»k ,=ð=miو ك½¤i,w ½ã>,ş› õ.ª,sa ➢و.ª ¾ ã=1Q2Sk c,,c=»k ¿¦,=í ,a ã=i,m£k ¿¦,=s»k ãí,,¤a
Qª=sa õ,k.> @é2=› ,Qu ½»kو ã1=ð=mSk õ,s¤»k ل5s £1=zSk 5Q£,i õ,k.£k ل,¤=ík õ,s,> y-22»k
«1w9í Qe,و õ,k.£k ل,¤=ík 5a,2a ¿a 5s Q=¤› ¸ 2g9Sk ,ij9-»k نí ãwk,2»k «ş=i ,Qs كãi2> ➢و.ªs
õ-د,ij ,a ل,¤=ík ل22a ¾ ª9z1a ¿ms 9i ãé,ge,i ã=şi.c=»k Q=¤»k ,a 2=c 53÷i «¤ék9; õ,s¤»k ل5s
كã=›9ð»k ¤í,>¿»k ل5s £xQ»k ¾ 2¤¤»k c,m> ¸ 1> «»›وذ õ,s¤»k ¾ ع,¤;,£k ãşmí